Journal of Nuclear Materials 385 (2009) 474–478

Contents lists available at ScienceDirect

Journal of Nuclear Materials

journal homepage: www.elsevier.com/locate/jnucmat

Thorium sorption onto magnetite and ferrihydrite in acidic conditions

I. Rojo [a,b,*], F. Seco [a], M. Rovira [a,b], J. Giménez [b], G. Cervantes [b], V. Martí [a,b], J. de Pablo [a,b]

[a] CTM Centre Tecnològic, Avda. de les Bases de Manresa 1, 08242 Manresa, Spain
[b] Chemical Engineering Department, Universitat Politècnica de Catalunya, Avda. Diagonal 647 H4, 08028 Barcelona, Spain

ARTICLE INFO

PACS:
68.43.−h
82.65.+r
28.41.K

ABSTRACT

Sorption of Th(IV) onto two-line ferrihydrite and magnetite in $NaClO_4$ solutions has been studied as a function of pH and ionic strength revealing that sorption onto both solids increases with pH while it is independent on ionic strength. Sorption capacity of both solids is high, the maximum sorption (almost 100% of Th(IV)) occurs at pH higher than 3.5 for ferrihydrite, and higher than 3.0 for magnetite. Sorption variation with pH was modeled with three different models using the FITEQL 4.0 code: non-electrostatic model, constant capacitance model, and diffuse-double layer model. In all cases, good fit to the experimental data is obtained with one-species: a corner-sharing bidentate-mononuclear surface complex, $(\equiv FeO)_2Th^{2+}$, which coincides with the surface complex postulated on these solids surface in previous spectroscopic studies; however, the monodentate species $\equiv FeOThOH^{2+}$ also gives a satisfactory fit. Under the experimental conditions of the present study, any effect of possible thorium colloid formation is negligible.

1. Introduction

An option for final disposal of high level radioactive waste is in a deep geological repository. The aim of disposal is to delay escape of radionuclides to the biosphere until their radiological impact is negligible [1]. In the repository, the radioactive waste is placed inside metallic containers, which represent the first physical barrier to radionuclide migration. However, a few hundreds years after emplacement the canister might fail due to iron corrosion [2] facilitating release of radionuclides to the geosphere. During corrosion of the canister, different Fe-containing corrosion products are formed, and they might affect the migration behaviour of a number of radionuclides through two different mechanisms: (1) iron corrosion can generate a reducing environment, which would keep many radionuclides in a less mobile form; and (2) corrosion products may immobilize certain radionuclides through sorption mechanisms.

One of the corrosion products of steel is magnetite (Fe_3O_4), which is reported to be the main stable end member of oxide transformations in moderate to strong reducing environments and neutral-alkaline conditions [3]. In addition, magnetite has been observed in previous experimental studies on steel corrosion in conditions simulating the repository [4]. Various studies have been performed examining the magnetite adsorption capacity for different actinides. Cui and Eriksen [5] studied the reduction and sorption of Np(V) on magnetite. U(VI) reduction and/or adsorption by magnetite has also been studied [6–9]. Powell et al. [10] characterized adsorption and reduction of PuO_2^+ by synthetic magnetite determining that reduction of Pu(V) occurs at all pH values (between 3 and 8). On the other hand, further intrusion of oxidants into the system may lead to the formation of Fe(III) oxides and hydroxides such as ferrihydrite. Ferrihydrite is a poorly ordered iron oxide hydroxide for which no general formula has been established [3]. This ‘amorphous’ oxide presents a high surface area which explains its larger sorption capacity for metal contaminants.

Interactions of radionuclides with magnetite and ferrihydrite should be evaluated to predict their retardation in the underground repositories. In particular, sorption of thorium onto iron oxides has not to date been studied in detail. Thorium in the context of radioactive disposal could increase in the future due to the use of new thorium-MOX fuels [11]. In addition, as a tetravalent ion it may be used as an analogue of other tetravalent actinides such as Np(IV) [12], U(IV) and Pu(IV) [13], which are difficult to retain in the tetravalent form.

Cromières et al. [14] made batch experiments of Th sorption onto hematite (α-Fe_2O_3) and studied the influence of pH (from 2 to 10) and ionic strength (from 0.01 to 0.1 M $NaClO_4$). Reiller et al. [15,16] studied the influence of humic acids on the retention of Th(IV) onto hematite and goethite (α-FeOOH). LaFlamme and Murray [17] and Hunter et al. [18] studied the sorption of Th onto goethite, and Murphy et al. [19] focused on the ternary system Th(IV)/marine colloid/hematite. Other studies deal with thorium sorption onto other oxides like silica [20–22], alumina [23,24], titania [25,26] or gibbsite [27]. In addition, Degueldre and Kline [28]

---

[*] Corresponding author. Address: CTM Centre Tecnològic, Avda. de les Bases de Manresa 1, 08242 Manresa, Spain. Tel.: +34 93 877 73 73; fax: +34 93 877 73 74.
E-mail address: isabel.rojo@ctm.com.es (I. Rojo).

0022-3115/$ - see front matter © 2008 Elsevier B.V. All rights reserved.
doi:10.1016/j.jnucmat.2008.12.014

developed a surface complexation model, based on the metal adsorption on free sites as well as on already contaminated sites, to simulate metal sorption on colloids and precipitation (polymerization) at their surface, and applied the model to reported experimental data of thorium onto FeOOH, Al_2O_3, TiO_2 and SiO_2. They also prove that polymerization at the surface cannot take place prior to *in situ* precipitation.

To our knowledge, thorium interaction with magnetite and ferrihydrite has not been studied. For this reason, the main objective of this work is to supply data on the adsorption of Th(IV) to two-line ferrihydrite and magnetite in the acidic pH range as well as to study the influence of the possible formation of thorium colloids on the sorption mechanism.

2. Experimental

2.1. Solids

The magnetite used in this work was supplied by Aldrich, with a purity of 98% and particle size less than 5 μm. Ferrihydrite used in the experiments was synthesized in house by precipitation with alkali according to the method described in [29]. Phases present in the solids were characterized by powder X-ray diffraction (XRD). Surface areas determined by the BET nitrogen adsorption method were 1.59 ± 0.01 $m^2 g^{-1}$, and 202 ± 3 $m^2 g^{-1}$ for magnetite and ferrihydrite, respectively.

2.2. Sorption experiments

Sorption experiments were conducted in 14-mL polystyrene tubes with 10 g L^{-1} of solid. The solution concentrations of Th(IV) were maintained below the solubility limit of amorphous ThO_2 [30]. Preliminary batch studies were conducted to assess the kinetics of Th sorption onto ferrihydrite and magnetite under different pH conditions (data not shown). Under the boundary conditions employed for these kinetic batch studies, an equilibrium contact time of 4 days was chosen for both solids.

All samples were centrifuged at 3000 rpm 10 min and filtered using 0.45 μm acetate cellulose filters. The filtrate was acidified and analysed with an ICP-MS (Perkin–Elmer 6000) to determine the bulk aqueous Th(IV) and Fe concentrations. Fe concentrations were determined to control the iron oxide dissolution. For the colloid formation study, the suspensions were, after 0.45 μm filtration, centrifuged at 3000 rpm for 90 min in 10 kDa centrifugal filters Centriplus® Amicon.

Concentration of sorbed thorium was determined by subtracting the remaining thorium concentration in the supernatant from the introduced thorium concentration.

3. Results and discussion

3.1. Variation of the thorium sorption with pH

The variation of thorium sorption with equilibrium pH in magnetite and ferrihydrite is shown in Fig. 1, where results of the samples filtered with cellulose filters and centrifugal ultrafilters are included. No large differences between the two filtration methodologies were detected suggesting that under the conditions of the present study, colloid formation does not influence the sorption phenomenon.

Fig. 1 shows that the thorium sorption edges are sharp sigmoid profiles characteristic of transition metals with pH_{50} ~2.2 and 2.9 for magnetite and ferrihydrite, respectively, which is consistent

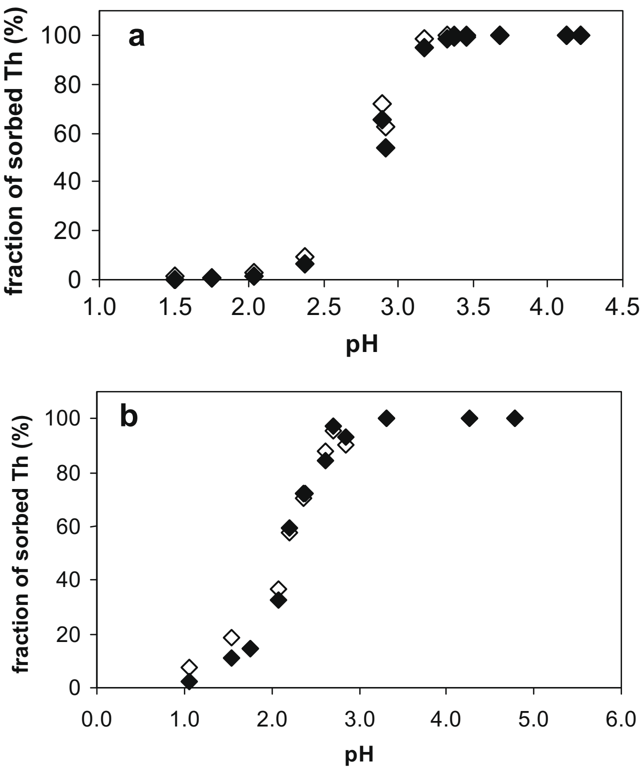

Fig. 1. Sorption of thorium as a function of pH at 10 g L^{-1}, $[Th]_{initial}$: 1.1 × 10^{-6} M and I = 0.1 M $NaClO_4$ for T = 298 K. Filled points: thorium concentrations measured after filtration at 450 nm, open points: thorium concentrations measured after ultrafiltration at 10 kDa. (a) Sorption onto ferrihydrite; (b) sorption onto magnetite.

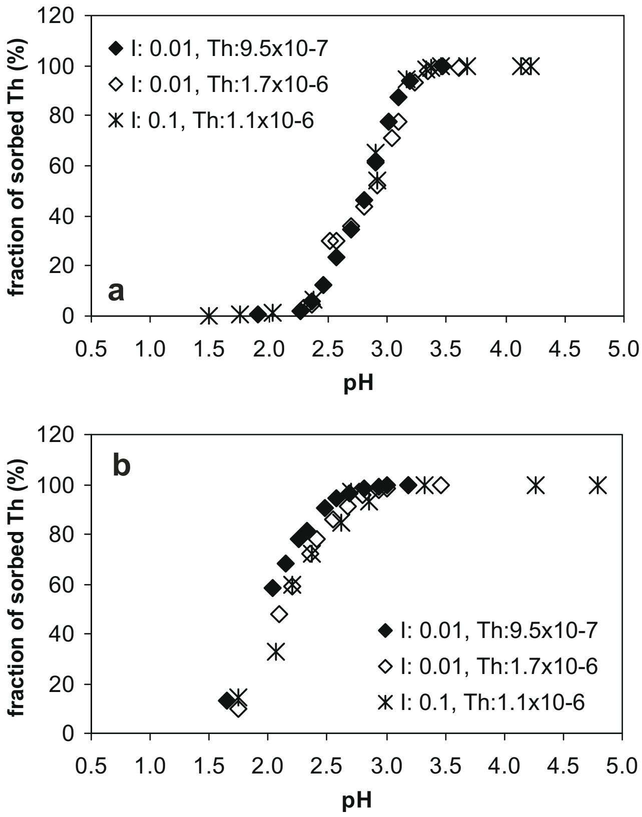

Fig. 2. Sorption of thorium as a function of pH at 10 g L^{-1} for T = 298 K. Ionic strength in $NaClO_4$ (M) and initial thorium concentration (M) are indicated inside the graphic. (a) Sorption on ferrihydrite, (b) sorption on magnetite.

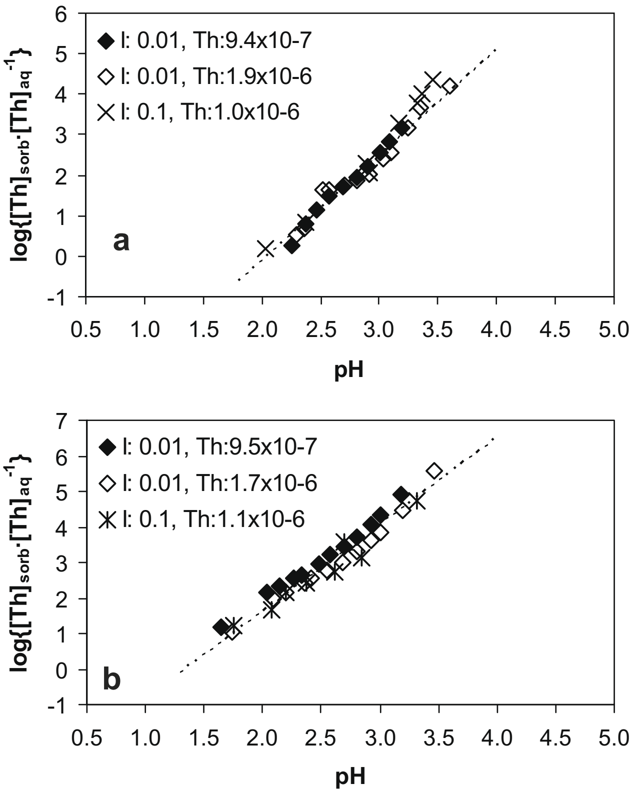

Fig. 3. Log–log plot of the pH edge for both solids. Dotted line represents a hypothetical straight line with slope 2. Experimental conditions of points are included in the graphic in M. (a) Ferrihydrite, (b) magnetite.

with the range observed for sorption of thorium on other oxides [19,21,23–25]. The maximal sorption is attained at pH 3 (magnetite) and 3.5 (ferrihydrite).

On the other hand, as it can be seen in Fig. 2, in the pH range studied, Th(IV) sorption to ferrihydrite and to magnetite is independent of ionic strength between 10^{-2} and 10^{-1} M $NaClO_4$, suggesting that this background electrolyte does not provide significant competition to Th(IV) sorption. These results suggest that Th(IV) primarily sorbs to ferrihydrite and magnetite to form inner-sphere complexes.

The sorption equilibrium reaction can be written as follows:

$$\mathrm{Th}^{4+} + n{\equiv}\mathrm{FeOH} + p\mathrm{H_2O} \leftrightarrow ({\equiv}\mathrm{FeO})_n\mathrm{Th(OH)}_p^{4-n-p} + (n+p)\mathrm{H}^+, \quad (1)$$

where $\equiv$FeOH describes one surface hydroxyl group and $(\equiv\mathrm{FeO})_n$ defines the number of surface hydroxyl groups reacting with a Th^{4+} cation. Thorium bound to surface hydroxyl groups connected to the same iron atom on the magnetite/ferrihydrite surface (edge sharing arrangement) or to surface hydroxyl groups connected to different, adjacent iron atoms (corner-sharing arrangement) and cannot be distinguished in this description.

The rearrangement of the expression for the sorption constant, K_s, corresponding to reaction (1) yields:

$$\log\frac{[\mathrm{Th}]_{\mathrm{sorb}}}{[\mathrm{Th}^{4+}]_{\mathrm{aq}}} = (n+p)\mathrm{pH} + \log K_{\mathrm{s}} + n\log[\mathrm{FeOH}]_{\mathrm{free}}, \quad (2)$$

where $[\mathrm{Th}]_{\mathrm{sorb}}$ represents the concentration of surface sorbed species, $(\equiv\mathrm{FeO})_n\mathrm{Th(OH)}_p^{4-n-p}$, and $[\mathrm{Th}^{4+}]_{\mathrm{aq}}$ the concentration of aqueous species in solution. Then a linear relationship exists between pH and $\log\frac{[\mathrm{Th}]_{\mathrm{sorb}}}{[\mathrm{Th}^{4+}]_{\mathrm{aq}}}$. The corresponding so-called 'log–log' plot is shown in Fig. 3.

The slope of the lines gives the total number of protons exchanged in the sorption process, $(n + p)$, where n gives the dentate character of the sorbed species and p defines the degree of hydrolysis. Only one region can be distinguished in Fig. 3 for both solids, the slope of the line in this region is ~2, which indicates that only one type of sorbed surface species is formed, and, in addition, the value of n and p can vary from 0 to 2. According to Bäes and Mesmer [31], thorium(IV) hydrolysis becomes detectable between pH 2 and 3. Moreover, Elyahyaoui et al. [32] observed that at trace levels, thorium hydrolysis seems to start at even lower pH (pH 1.2). Since the slope in the log–log plot is determined within the pH range 1.65–3.60, the possibility of $p = 0$ cannot be excluded. Therefore, three options are possible: (1) $p = 2$ and $n = 0$, corresponding to thorium hydrolysis with no thorium adsorption onto the hydroxyl groups of iron oxides, (2) $p = 1$ and $n = 1$, the combination values expected for formation of a monodentate species ($\equiv\mathrm{FeOThOH}^{2+}$) without hydrolysis, and finally, (3) $p = 0$ and $n = 2$, the values expected for formation of a bidentate species ($(\equiv\mathrm{FeO})_2\mathrm{Th}^{2+}$) without hydrolysis.

3.2. Modeling thorium sorption on ferrihydrite and magnetite

To model the formation of surface complexes on magnetite and ferrihydrite, the FITEQL 4.0 program was used [33]. Three different surface complexation models (SCM) that differ in the description of the interfacial region were used to model the experimental data: the non-electrostatic model (NEM), the constant capacitance model (CCM) and the diffuse layer model (DLM). The application of a SCM by using the FITEQL code requires a number of parameters such as the specific surface area (A_s) of the solids, the concentration

Table 1
Hydrolysis constants for Th and acidity constants for magnetite and ferrihydrite used in this work to fit experimental data at 298 K.

Reactions	Log *K* (*I* = 0)		Reference
$Th^{4+} + H_2O \leftrightarrow Th(OH)^{3+} + H^+$	−2.2		[30]
$Th^{4+} + 2H_2O \leftrightarrow Th(OH)_2^{2+} + 2H^+$	−6.6		[30]
$Th^{4+} + 3H_2O \leftrightarrow Th(OH)_3^{+} + 3H^+$	−11.4		[30]
$Th^{4+} + 4H_2O \leftrightarrow Th(OH)_4 + 4H^+$	−17.0		[30]
$2Th^{4+} + 2H_2O \leftrightarrow Th_2(OH)_2^{6+} + 2H^+$	−5.7		[34]
$4Th^{4+} + 8H_2O \rightarrow Th_4(OH)_8^{8+} + 8H^+$	−20.4		[34]
$4Th^{4+} + 12H_2O \leftrightarrow Th_4(OH)_{12}^{4+} + 12H^+$	−26.7		[34]
$6Th^{4+} + 15H_2O \leftrightarrow Th_6(OH)_{15}^{9+} + 15H^+$	−34.0		[34]
Magnetite	Log *K* (*I* = 0.1)	Log *K* (*I* = 0.01)	
$FeOH_2+ \leftrightarrow FeOH + H^+$	−5.8	−5.4	[35]
$FeOH \leftrightarrow FeO^- + H^+$	−9.1	−9.5	[35]
Ferrihydrite	Log *K* (*I* = 0)		
$FeOH_2^+ \leftrightarrow FeOH + H^+$	−7.29		[36]
$FeOH \leftrightarrow FeO^- + H^+$	−8.93		[36]

of surface adsorption sites (N_s), the acidity constants of ≡FeOH sites (K_+ and K_-), and the thermodynamic constants for thorium hydrolysis complexes. These are literature parameters (see Table 1) except the solids specific surface areas, which were determined experimentally. The density of surface sites value was the one given by Davis and Kent [37], 2.31 nm^{-2}. In the CCM and DLM, a value of 1.2 F m^{-2} for the surface capacitance was chosen, according to [38]. The Debye–Hückel equation [39] was used to calculate the acidity constants at the appropriate ionic strength.

Recent X-ray absorption fine structure spectroscopy (XAFS) investigations [40] seem to indicate that the dominant sorption mechanism is the formation of a corner-sharing bidentate surface species. In addition, inner-sphere versus outer-sphere surface complex formation has been inferred from the impact of ionic strength on sorption (see above). Thus, the modeling of the sorption edge data was first done considering the formation of a corner-sharing bidentate-mononuclear inner-sphere surface complex.

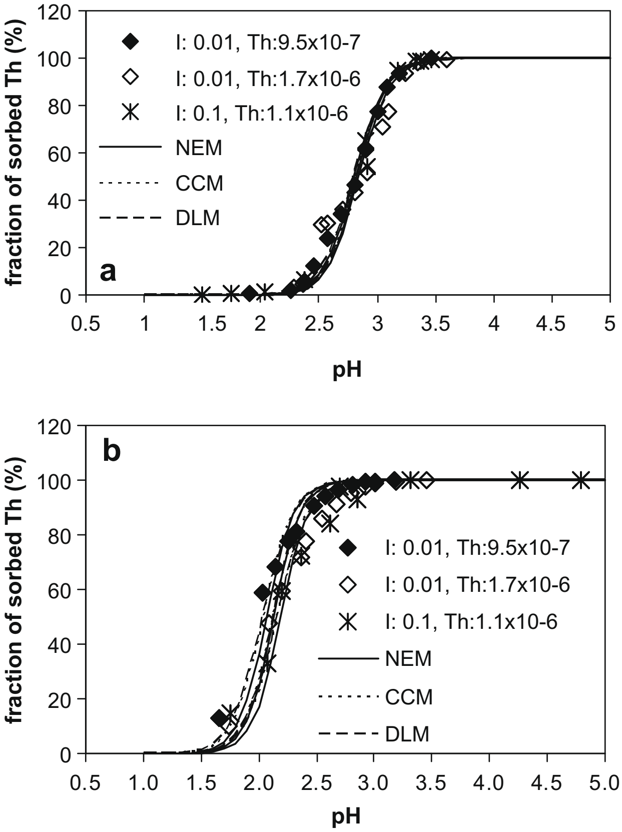

Fig. 4. Sorption of thorium as a function of pH at sorbing concentration of 10 g L^{-1}. Ionic strength in NaClO$_4$ (M) and initial thorium concentration (M) are indicated inside the graphic. Lines: optimized fits using a $(\equiv FeO)_2Th^{2+}$ species and NEM, CCM and DLM models. (a) Ferrihydrite, (b) magnetite.

Table 2
NEM, CCM and DLM sorption constants (standard deviations in parenthesis) from experimental data for thorium adsorption to ferrihydrite and magnetite at 298 K.

I (M)	[Th]$_{initial}$ (M)	Log K_{NEM}	Log K_{CCM}	Log K_{DLM}
Ferrihydrite				
0.1	1.1×10^{-6}	7.57 (1.25)	7.84 (1.25)	7.59 (1.25)
0.01	9.4×10^{-7}	8.09 (1.02)	8.33 (1.00)	8.19 (0.99)
0.01	1.9×10^{-6}	7.98 (0.51)	8.22 (0.50)	8.08 (0.50)
Magnetite				
0.1	1.1×10^{-6}	11.61 (1.29)	12.00 (1.28)	11.68 (1.28)
0.01	9.4×10^{-7}	11.13 (1.33)	11.66 (1.29)	11.67 (1.26)
0.01	1.9×10^{-6}	10.69 (0.72)	11.25 (0.70)	11.29 (0.67)

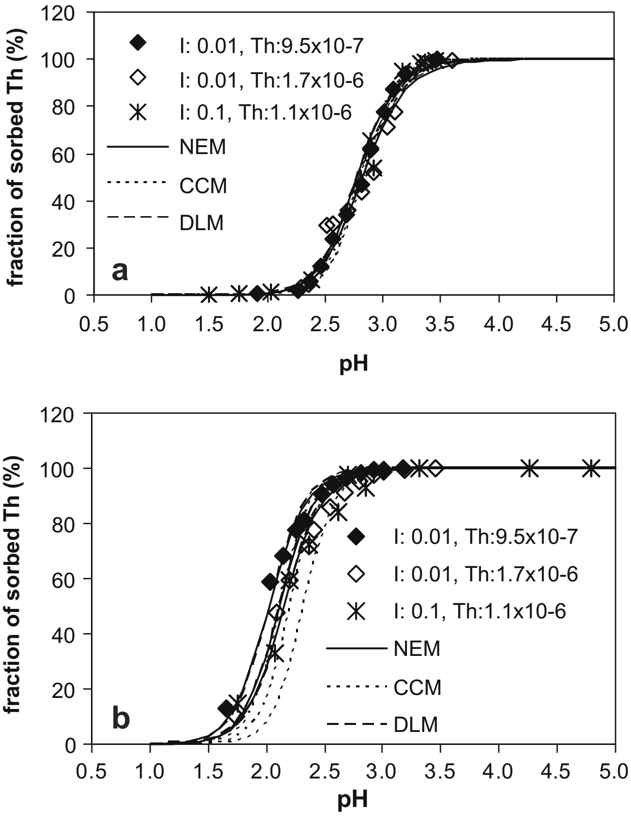

Fig. 5. Sorption of thorium as a function of pH at sorbing concentration of 10 g L^{-1}. Ionic strength in NaClO$_4$ (M) and initial thorium concentration (M) are indicated inside the graphic. Lines: optimized fits using a $\equiv FeOThOH^{2+}$ species and NEM, CCM and DLM models. (a) Ferrihydrite, (b) magnetite.

Modeling of the thorium(IV) sorption onto ferrihydrite and magnetite is shown in Fig. 4, which includes the NEM, CCM and DLM fits obtained using the corner-sharing bidentate-mononuclear surface complex $(\equiv FeO)_2Th^{2+}$. Table 2 includes the optimized equilibrium constants and associated standard deviation values for the different sorption edges fits. Equilibrium constants for the bidentate-mononuclear Th(IV) surface complex are reported as conditional K values (K_i), rather than as intrinsic K values (K_i^{int}), because of the dependence on ionic strength.

For both solids, all the three tested surface complexation models give a similar and satisfactory fits to the experimental data, suggesting that the fit quality and the surface complexation constants obtained when considering a bidentate stoichiometry do not depend strongly on the electrostatic term. In other words, this seems to indicate that the surface reaction is not influenced by the presence or the shape of an electrostatic layer.

The species $\equiv FeOThOH^{2+}$ provided essentially the same fitting as the bidentate surface complex (Fig. 5). Mathematically, the mass law expression for $\equiv FeOThOH^{2+}$ looks very similar to the mass law expression for $(\equiv FeO)_2Th^{2+}$. In addition, a combination of two surface species, a monodentate and a bidentate, in the FITEQL optimization was tested with no convergence of the program.

4. Conclusions

Sorption of thorium on synthetic two-line ferrihydrite and commercial magnetite was studied under oxidising conditions. Previous kinetics sorption studies showed that 4 days contact time was enough to reach equilibrium.

The sorption edges of Th onto magnetite and ferrihydrite are independent on the ionic strength and are characterized by a pH_{50} ~2.2 and 2.9 for magnetite and ferrihydrite, respectively. Under the conditions of this work, colloids do not affect the sorption phenomenon.

The graphical 'log–log' plot approximation in the pH range 1.65–3.60 indicates that only one type of sorbed surface species is formed at acidic pH, likely being either a monodentate or bidentate specie with the corresponding release of two protons. Previous EXAFS results (give reference) proposed that the sorbed specie is a bidentate complex with Th bonded via a corner-sharing arrangement. The insights provided by the pH sorption edge data are consistent with the spectroscopic findings.

Sorption data were successfully modelled with the NEM, CCM and DLM models considering a single bidentate complex and one type of surface site. However, good fitting is also obtained considering a single monodentate complex. These results could indicate that there are some local bidentate surface complexes but without excluding the presence of monodentate surface complexes.

Acknowledgements

Financial support for this research was provided by ENRESA (Spanish Radioactive Waste Management Co.) in the framework of the European Commission FUNMIG project (Fundamental processes of radionuclide migration) and the Spanish 'Ministerio de Educación y Ciencia' by means of the 'Juan de la Cierva' and 'Ramon y Cajal' programs and the AMAME project (Contract number: CTM2005-07037-C03-01/TECNO), as well as the support of the program 'Beatriu de Pinós' d'ACC1Ó from the Generalitat de Catalunya.

References

[1] N.A. Chapman, I.G. McKinley, The Geological Disposal of Nuclear Waste, Wiley-Interscience, New York, 1987.
[2] A.R. Hoch, A. Honda, F.M. Porter, S.M. Sharland, N. Taniguchi, in: Materials Research Society Symposium Proceedings, vol. 465, Published MRS, Pittsburg, 1997, p. 683.
[3] R.M. Cornell, U. Schwertmann, The Iron Oxides, VCH, New York, 1996.
[4] B. Grambow, E. Smailos, H. Geckeis, R. Mueller, H. Hentschel, Radiochim. Acta 74 (1996) 149–154.
[5] D. Cui, T.E. Eriksen, Reduction of Tc(VII) and Np(V) in solution by ferrous ion. A laboratory study of homogeneous and heterogeneous redox processes. SKB Technical Report TR-96-03, Stockholm, Sweden, 1996.
[6] S. El Aamrani, J. Giménez, M. Rovira, F. Seco, M. Grivé, J. Bruno, L. Duro, J. de Pablo, Appl. Surf. Sci. 253 (2007) 8794–8797.
[7] T. Missana, C. Maffiotte, M. García-Gutiérrez, J. Colloid Interface Sci. 261 (2003) 154–160.
[8] M. Rovira, S. El Aamrani, L. Duro, J. Giménez, J. de Pablo, J. Bruno, J. Hazard. Mater. 147 (2007) 726–731.
[9] L. Duro, S. El Aamrani, M. Rovira, J. de Pablo, J. Bruno, Appl. Geochem. 23 (2008) 1094–1100.
[10] B.A. Powell, R.A. Fjeld, D.I. Kaplan, J.T. Coates, S.M. Serkiz, Environ. Sci. Technol. 38 (2004) 6016–6024.
[11] J. Cobos, J. Quiñones, C. Kütahyali, V.V. Rondinella, J. Somers, R. Konings, Determination of the Th-MOX inventory leached out in contact with water, in: Proceedings of the 11th International Conference on the Chemistry and Migration Behavior of Actinides and Fission Products in the Geosphere (Migration'07) München (Germany) 26–31 August 2007.
[12] C. Degueldre, J. Environ. Radioact. 29 (1995) 75–87.
[13] G.R. Choppin, Radiochim. Acta 85 (1999) 89–95.
[14] L. Cromières, V. Moulin, B. Fourest, R. Guillaumont, E. Giffaut, Radiochim. Acta 82 (1998) 249–255.
[15] P. Reiller, F. Casanova, V. Moulin, Environ. Sci. Technol. 39 (6) (2005) 1641–1648.
[16] P. Reiller, V. Moulin, F. Casanova, C. Dautel, Appl. Geochem. 17 (2002) 1551–1562.
[17] B.D. LaFlamme, J.W. Murray, Geochim. Cosmochim. Acta 51 (1987) 243–250.
[18] K.A. Hunter, D.J. Hawke, L. Kwee Choo, Geochim. Cosmochim. Acta 52 (1988) 627–636.
[19] R.J. Murphy, J.J. Lenhart, B.D. Honeyman, J. Colloid Surf. A 157 (1999) 47–62.
[20] E. Östhols, A. Manceau, F. Farges, L. Charlet, J. Colloid Interface Sci. 194 (1997) 10–21.
[21] E. Östhols, Geochim. Cosmochim. Acta 59 (1995) 1235–1249.
[22] C. Chen, X. Wang, Appl. Radiat. Isot. 65 (2007) 155–163.
[23] C.L. Chen, X.K. Wang, Appl. Geochem. 22 (2007) 436–445.
[24] L. Righetto, G. Bidoglio, B. Marcandalli, I.R. Bellobono, Radiochim. Acta 44/45 (1988) 73–75.
[25] A.M. Jakobsson, J. Colloid Interface Sci. 220 (1999) 367–373.
[26] X. Tan, X. Wang, C. Chen, A. Sun, Appl. Radiat. Isot. 65 (2007) 375–381.
[27] H. Zhang, D. Zheng, Z. Tao, Colloids Surf. A: Physicochem. Eng. Aspects 278 (2006) 46–52.
[28] C. Degueldre, A. Kline, Earth Planet. Sci. Lett. 264 (2007) 104–113.
[29] U. Schwertmann, R.M. Cornell, Iron Oxides in the Laboratory: Preparation and Characterization, VCH, Weinheim, 1991.
[30] M. Altmaier, V. Neck, R. Müller, Th. Fanghänel, Radiochim. Acta 93 (2005) 83–92.
[31] C.F. Bäes, R.E. Mesmer, The Hydrolysis of Cations, Wiley-Interscience Publication, New York, 1976. p. 158.
[32] A. Elyahyaoui, L. Brillard, S. Boulhassa, M. Hussonnois, R. Guillaumont, Radiochim. Acta 49 (1990) 39–44.
[33] A.L. Herberli, J.C. Westall, FITEQL: A Computer Program for the Determination of Chemical Equilibrium Constants from Experimental Data, Chemistry Department, Oregon State University, Corvallis, OR, 1999.
[34] V. Neck, R. Müller, M. Bouby, M. Altmaier, J. Rothe, M.A. Denecke, J.I. Kim, Radiochim. Acta 90 (2002) 485–494.
[35] D.A. Sverjensky, N. Sahai, Geochim. Cosmochim. Acta 60 (1996) 3773–3797.
[36] D.A. Dzombak, F.M.M. Morel, Surface Complexation Modeling: Hydrous Ferric Oxide, Wiley, New York, 1990.
[37] J.A. Davis, D.B. Kent, Surface complexation modeling in aqueous geochemistry, in: Hochella, White (Eds.), Mineral-water Interface geochemistry, Min. Soc. Amer. Rev. Mineral. 23 (1990) 177.
[38] N. Marmier, A. Delisée, F. Fromage, J. Colloid Interface Sci. 211 (1999) 54–60.
[39] I. Grenthe, I. Puigdomenech, Modelling in Aquatic Chemistry, OECD Publications, 1997. p. 724.
[40] F. Seco, C. Hennig, J. de Pablo, M. Rovira, I. Rojo, V. Martí, J. Giménez, L. Duro, M. Grivé, J. Bruno, Environ. Sci. Technol., submitted for publication.